

**Compensating the influence of the Earth's Magnetic
Field on the scintillator detector resolutions by
PMTs orientation**

A. Ianni^a, G. Korga^b, G. Ranucci^b, O. Smirnov^{b,c}, A. Sotnikov^{b,c}

Compensating the influence of the Earth's Magnetic Field on the scintillator detector resolutions by PMTs orientation

A. Ianni^a, G. Korga^b, G. Ranucci^b, O. Smirnov^{b,c}, A. Sotnikov^{b,c}

^a *Department of Physics, Princeton University, 08544-0708 Princeton - NJ, USA*

^b *INFN Sezione di Milano, Via Celoria (Mi) - Italy*

^c *Nuclear Research, J. Curie 6, 141980 Dubna - Russia*

Abstract

The two common ways implemented to compensate the Earth's Magnetic Field (EMF) in a large volume scintillator detector are either a μ -metal shielding of photomultipliers (PMTs) or an overall geomagnetic field compensation by a complex coil-system. As a matter of fact a PMT is mainly sensitive to the field component which is parallel to the dynodes. This effect provides the possibility to align properly the PMTs with respect to the EMF in order to decrease the degradation of its performances. In this article we present a quantitative estimation of the possible effect on the energy and spatial resolutions for this solution. The PMT under test is the 8" ETL9351.

1 Introduction

Large scale liquid scintillator detectors such as BOREXINO [1, 2] (or its prototype CTF [3, 4]) are using wide area photocathode PMTs that are extremely sensitive to the presence of the Earth's Magnetic Field (EMF) [5]. Two standard ways to compensate the EMF have been used so far in different experiments: a PMT screening with a metal with high magnetic permeability (μ -metal), and a magnetic field compensation using a properly designed coil-system (i.e. in SuperKamiokande the residual geo-magnetic field is kept less than 100mG in every position of the tank by using compensation coils [6]). The possibility to use a circular coil-system for the EMF compensation has been studied for Borexino as well [7]. However, in BOREXINO finally it was decided to use μ -metals as passive system to shield PMTs against the EMF.

Both these methods have their disadvantages. The usage of a μ -metal in a high purity detector, such as BOREXINO, for example, introduces an additional amount of material that is a possible source of radioactive contamination. Another problem is, eventually, the chemical incompatibility between the μ -metal and the scintillator. Furthermore, it often turns out that not all the PMTs can be installed with a μ -metal and in this case an alternative solution to compensate the EMF is needed. In BOREXINO, as an example, many muon-veto PMTs are installed together with a tyvek plate around the photocathode for light collection purposes and there is not enough room to mount a μ -metal. On the other hand as far as a coil-system is concerned, we have to deal with the problem to compensate the EMF in a very large volume. This problem is not always straightforward to figure out. In many cases we could have problems in compensating all the volume we are interested in because of a not homogeneous EMF.

In this article an alternative procedure of the EMF compensation by a PMT orientation in the EMF is studied.

The plan of the paper is as follows. We describe the experimental setup and measurements in Section 2. In Section 3 and 4 we estimate the effect of the alignment on the energy resolution and on the transit time and spatial reconstruction, respectively. In Section 5 we quantify the effect of the accuracy on the PMT orientation. In Section 6 we underline few practical issues to take into account during the installation of the PMTs in the case some of them have to be aligned. In Section 7 we draw our conclusions.

2 Experimental setup and measurements

For the data taking the PMTs test facility of BOREXINO at the Gran Sasso Laboratory, Italy, has been used (for details see [8]). In this test facility it is possible to set the value of the magnetic field (and its direction with respect to the dynodes of the PMT) using a coil-system [5]. By using this facility we measured the Single Electron Response (SER) and we simulated as an example of a real detector the CTF conditions [3]. In the CTF there are 100 PMTs looking at a nylon vessel filled with scintillator. So, each scintillation event is the convolution of 100 signals from different PMTs. In our simulation a special subroutine was realized for filling the "energy" histogram with the sum of 100 consequent

events. The mean photoelectrons (p.e.) number, μ , was set to approximately 1.6 in order to simulate a $160/330=0.5$ MeV event in the CTF¹.

In Figure 1 the charge spectra for the case of the compensated magnetic field are shown. The data have been taken simultaneously in such a way that all the parameters estimated are the same for both histograms.

Together with the charge spectrum, the transit time spread was acquired, with the discriminator threshold set at the level of 0.2 p.e., or 20% of the mean value of the SER.

The measurements in the magnetic field were performed for the following field orientations with respect to the PMT dynodes system (see Figure 2 for the axes choice):

1. completely compensated EMF;
2. field along +/- **Y** axis of PMT;
3. field along +/- **X** axis of PMT;
4. field along +/- **Z** axis of PMT.

It was found that the position of the gaussian depends upon the field orientation. A PMT high voltage adjustment was performed for each case, when the deviation with respect to the position of the gaussian in the completely compensated scenario was at the level of few % (in order to restore the mean PMT gain at $k=10^7$). All SER parameters were measured after the high voltage adjustment. Then the compensated SER conditions were restored and new measurements were carried out to avoid any possible systematic error.

Two 8" ETL9351 PMTs were tested, both of them demonstrated the same behaviour against the magnetic field.

3 Influence of the magnetic field on the energy resolution

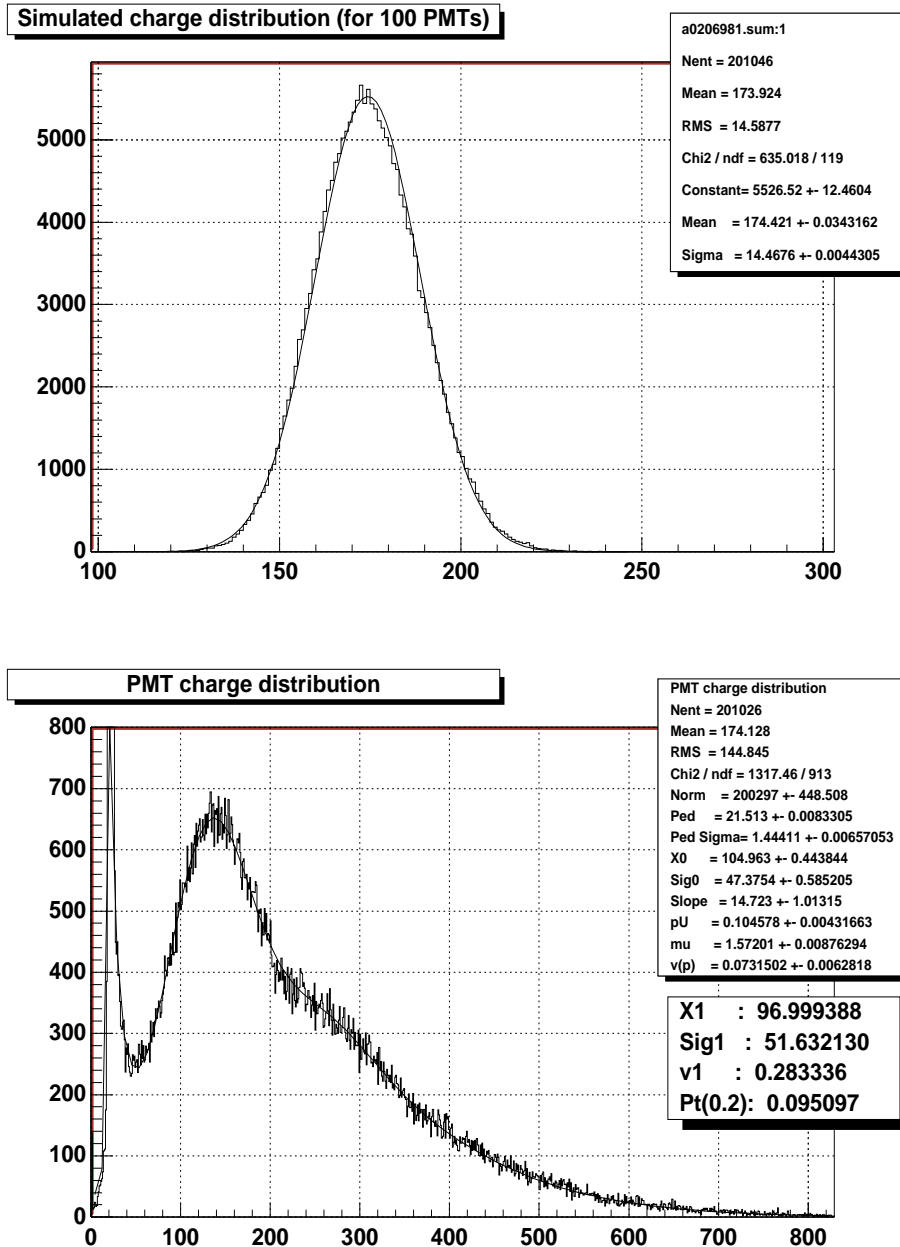
The data taken with the setup described in the previous Section are presented in the table 1. In particular, only the data for the adjusted HV are presented (the data without HV adjustment are the same within the measurements precision). The first column of table 1 presents the magnetic field components measured in units of the EMF (about $40 \mu T$)².

The resolution (second column) was defined as σ/X_0 using the fitting gaussian parameters. This is the main parameter of interest for the energy reconstruction. It could be seen from the data that the energy resolution is almost insensitive to the **X** and **Z** components of the EMF (deviations are within 6%).

¹330 p.e. per MeV were observed in the CTF [3]

²An absolute value of about $40 \mu T$ was measured for the EMF in the underground experimental Hall C of the Gran Sasso Laboratory, where BOREXINO is located. The deviation of the EMF with respect to a vertical alignment is about 40 degrees.

Figure 1: PMT charge spectra in the compensated magnetic field. The upper spectrum shows a simulation of the CTF conditions (100 PMTs, event energy 0.5 MeV), the lower one corresponds to a mean p.e. number of 1.6. The spectra were acquired in parallel, so their parameters are the same. The shape of the upper spectrum is close to a gaussian, this makes it convenient for the tuning of the PMT gain. The detector resolution can be defined in a very simple way from this spectrum as σ_Q/Q_0 .



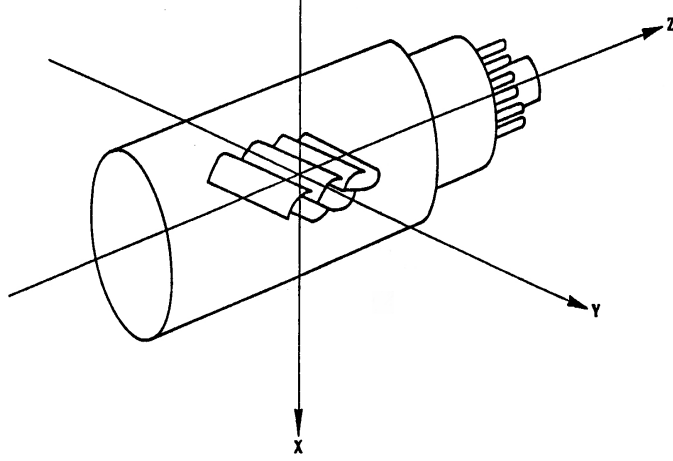


Figure 2: Axes choice for the linear focusing dynodes system of the 8" ETL9351 PMT.

Table 1: PMT SER parameters in the magnetic field. See text for details.

Field			PMT parameters					
H_x	H_y	H_z	Res(%)	$\Delta(HV)$	μ_0	$\mu(H)$	I(H)	v_1
0	0	0	9.5		1.64		1.00	0.31
-1	0	0	9.8	+11	1.57	1.48	0.94	0.31
+1	0	0	9.7	+9	1.58	1.50	0.95	0.31
0	-1	0	11.1	+106	1.57	1.24	0.79	0.44
0	+1	0	12.7	+60	1.57	1.14	0.73	0.71
0	0	-1	9.9	+15	1.56	1.48	0.95	0.36
0	0	+1	10.1	+17	1.52	1.43	0.94	0.37

In table 1 $\Delta(HV)$ is the high voltage change needed to restore the PMT gain and it is measured in units of Volts.

Together with the resolution, the mean p.e. number was estimated for the each case (the method is described in [8]). In particular, μ_0 and $\mu(H)$ are the mean number of p.e. in the compensated and not compensated field, respectively. The relative PMT sensitivity, defined as $I(H) = \mu(H)/\mu_0$, is presented in the same table. The relative sensitivity was estimated taking as reference point the p.e. number, μ_0 , for the compensated field.

The last column in the table1 presents the relative variance v_1 of the SER. This parameter, and the relative intensity $I(H)$, can be used to estimate the distortion of the energy resolution due to the magnetic field. As it is shown in [10] the detector energy resolution $R(E)$ is:

$$R(E) = \sqrt{\frac{1 + v_1^{det}}{Q(E)}}, \quad (1)$$

where $Q(E)$ is the mean p.e. number registered in an event of energy E and v_1^{det} is the PMT parameter v_1 (relative variance of the SER signal) averaged over all the PMTs (N_{ch}). Taking into account the relative sensitivity of each PMT, s_i (PMT sensitivity divided by the average sensitivity), we can write:

$$v_1^{det} \equiv \frac{1}{N_{ch}} \sum_{i=1}^{N_{ch}} v_{1_i} s_i.$$

For our purpose it is enough to know the deviation from the expected resolution in the presence of the EMF. The data from table 1 can be used:

$$\frac{R_H(E)}{R_0(E)} = \sqrt{\frac{1 + v_1^{det}(H)}{(1 + v_1^{det}(H=0)) \cdot I(H)}}, \quad (2)$$

where $R_H(E)$ and $v_1^{det}(H)$ are the energy resolution and averaged SER relative variance in the presence of the magnetic field, respectively, and $R_0(E)$ and $v_1^{det}(H=0)$ the energy resolution and averaged SER relative variance in the completely compensated field.

One can check that the data for the Resolution in table1 follow rigorously the law in (2).

The μ -metal shielding along the \mathbf{Z} axis was investigated in [9]. The sensitivity was found to be in the range 0.96-0.97 in comparison to the case of compensated field. Together with the data reported in table 1 (the relative sensitivity is 0.95 and 0.94 for the field direction along \mathbf{Z} and in the opposite direction correspondingly) this means that the μ -metal shielding is not effective along the \mathbf{Z} direction.

The worst case of $\mathbf{Y}+$ component shows about a 30% degradation of the resolution in comparison to the ideal case in a compensated magnetic field (12.7% instead of 9.5% for 160 p.e. that corresponds to 500 keV energy deposition in the CTF). If all the PMTs were aligned in such a way that the \mathbf{Y} component is compensated, the resolution would degrade down to 10.1% due to the uncompensated $\mathbf{Z}+$ of the magnetic field (the influence

Table 2: *PMT transit time parameters in the presence of a Magnetic Field*

Field			PMT parameters					
H_x	H_y	H_z	$p_t(H = 0)$	$p_t(U = U_0 + \Delta U)$	$I_t(H)$	$I_t \times I(H)$	σ_{TT}	TT tail
0	0	0	0.110	0.106	1.00	0.94	1.56	0.15
-1	0	0	0.110	0.106	1.00	0.94	1.56	0.15
+1	0	0	0.118	0.115	1.00	0.95	1.57	0.14
0	-1	0	0.125	0.166	0.96	0.76	1.60	0.285
0	+1	0	0.125	0.279	0.82	0.65	1.76	0.195
0	0	-1	0.118	0.134	0.98	0.93	1.51	0.175
0	0	+1	0.121	0.141	0.97	0.91	1.52	0.175

of all other components is negligible, as it can be seen from table 1). As it was already mentioned, a μ -metal is not effective in this orientation, so we will not consider the influence of the EMF along the **Z**- component on the signal.

Having the PMT aligned in such a way that the field along the **Y** axis is minimum, the maximum degradation of the resolution (in the worst case of the maximum presence of the **X**- component) is only about 5%. The real degradation will be even less due to the averaging of the components.

The same data as reported above were acquired with a 50% transparent filter (i.e. two times less light). All the measured parameters follow a direct proportionality law against the mean number of the registered p.e. μ (or the gaussian mean value $\langle x \rangle$, considering the described simulation).

4 Influence of the magnetic field on the spatial reconstruction

The EMF also affects the transit time spread of a PMT. Therefore, we studied the influence of the magnetic field on this parameter by measuring the transit time distribution.

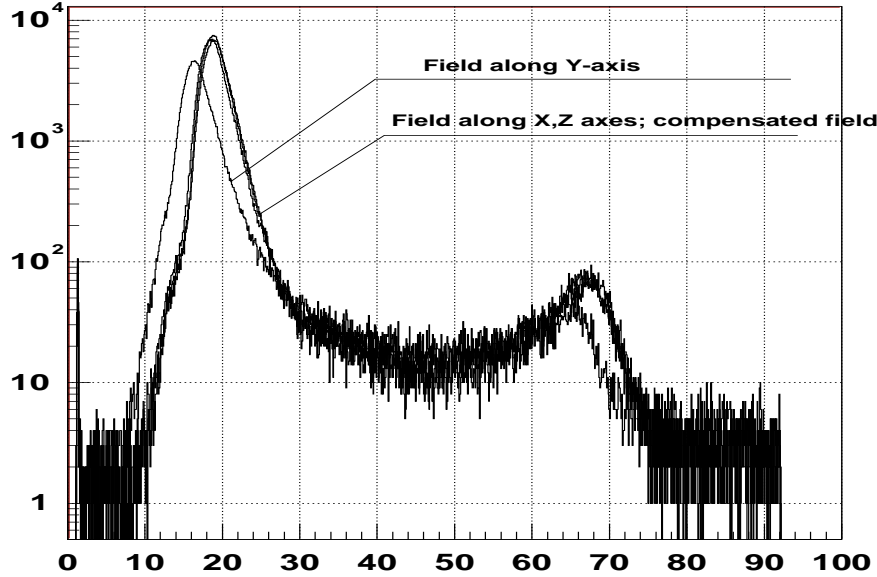
The transit time spread was studied under the same conditions as before. In Figure 3 the transit time spread histograms for all the three field orientations are shown. It could be seen that only the Y component significantly influences the transit time behaviour.

The transit time is obtained with the threshold set at 0.2 p.e. as it was mentioned in Section 2. This scenario is different with respect to the case of the energy measurements because of an additional cut of the small amplitude pulses. Therefore, in order to estimate the relative sensitivity it is necessary to take into account the fraction of the SER under the threshold.

In table 2 the data, obtained with the SER model described in [8], are presented. The relative PMT sensitivity at 0.2 p.e. threshold level has been defined as:

$$I_t(H) = \frac{1 - p_t(H)}{1 - p_t(0)},$$

Figure 3: The transit time for different orientations of the magnetic field.



where p_t is the fraction of the SER signals under the threshold.

The relative sensitivity of the PMT to the signals with amplitude greater than 0.2 p.e. can be defined as the product $I_t \times I(H)$, where $I(H)$ is the PMT relative sensitivity μ/μ_0 from the previous Section.

The last two columns present the transit time spread (the sigma of the gaussian fitting the transit time distribution, in ns) and the relative amount of pulses in the non-gaussian tail (late pulses). The latter have been defined as the ratio of the number of the events arrived after $t_0 + 3\sigma_{TT}$ to the number of events in the main peak. One can see that the transit time spread remains almost unchanged while the amount of late pulses increases slightly for the case of the **Z**- component and is much bigger for the **Y**- component.

As in the case of the spatial resolution estimations the values for the field along the Z axis should be compared to the PMT inside the μ -metal shielding. The expected decrease of sensitivity is about 6% for both axes (**X** and **Z**).

The spatial resolution at low energies is inversely proportional to the number of hit PMTs in the event[10]. This latter is proportional to μ , the mean number of the p.e. registered in an event³. At high energies, the resolution is insensitive to the fluctuations of the mean number of the registered p.e. So, one can write for the low energy event:

³Here a low energy event is defined in term of the mean number of registered p.e., which strongly depends on the detector geometry and light yield. For example, a 50 keV event in the CTF can be considered as a “low energy” one, because it results in 0.17 p.e. for the single PMT. In Borexino this limit is much higher. In particular, with 2200 PMTs and 400 p.e./MeV the same p.e number for PMT corresponds to a 1 MeV event.

Table 3: PMT sensitivity to the EMF Y-component (charge distribution effect)

Field			The PMT parameters			
H_x	H_y	H_z	μ	v_1	$\mathbf{I}(\mathbf{H})$	$R_H(E)/R_0(E)$
0	0	0	0.264	0.34	1.00	1.00
0	0.1	0	0.261	0.38	0.99	1.02
0	0.2	0	0.251	0.42	0.95	1.05
0	0.3	0	0.244	0.48	0.93	1.09
0	0.4	0	0.221	0.56	0.84	1.18
0	0.6	0	0.200	0.73	0.76	1.31
$\frac{1}{\sqrt{2}}$	0	$\frac{1}{\sqrt{2}}$	0.254	0.34	0.96	1.02

Table 4: PMT sensitivity to the EMF Y-component (transit time effect)

Field			The PMT parameters				
H_x	H_y	H_z	$p_t(H)$	$I_t \times I(H)$	$R_H(\vec{r})/R_0(\vec{r})$	σ_{TT}	TT tail
0	0	0	0.14	1.00	1.00	1.09	0.196
0	0.1	0	0.16	0.97	1.02	1.11	0.199
0	0.2	0	0.18	0.90	1.05	1.12	0.196
0	0.3	0	0.21	0.86	1.08	1.15	0.203
0	0.4	0	0.23	0.76	1.15	1.18	0.214
0	0.6	0	0.29	0.63	1.26	-	-
$\frac{1}{\sqrt{2}}$	0.	$\frac{1}{\sqrt{2}}$	0.14	0.96	1.02	-	-

$$\frac{R_H(\vec{r})}{R_0(\vec{r})} = \sqrt{\frac{\frac{1}{\mu(H)}}{\frac{1}{\mu(Shield)}}} = \sqrt{\frac{I(Shield)}{I(H)}} = \sqrt{\frac{0.96}{0.91}} = 1.03 \quad (3)$$

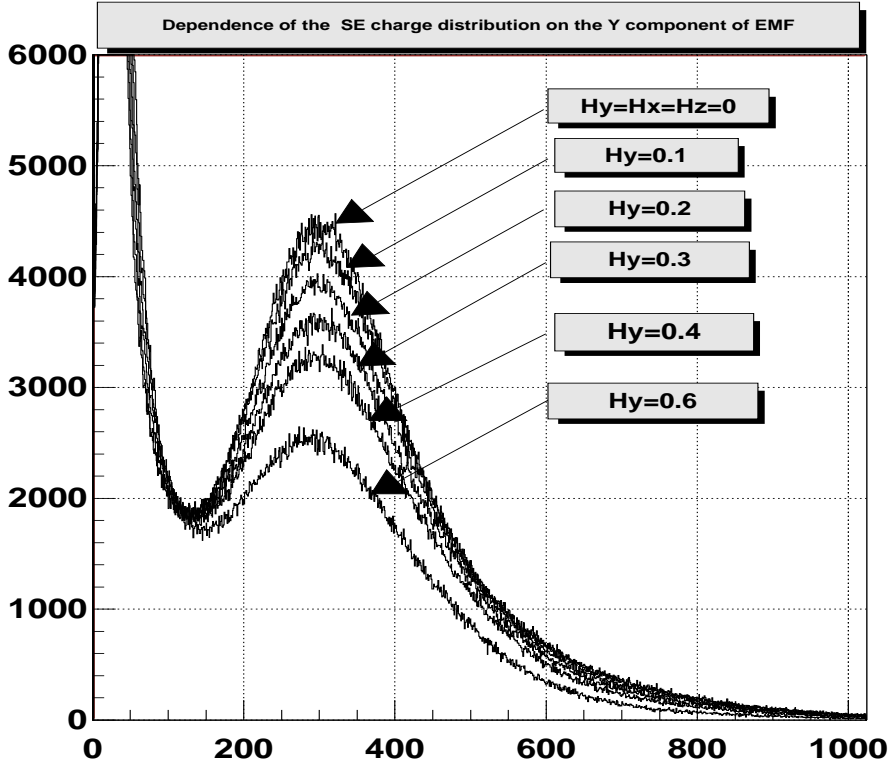
where $R_0(\vec{r})$ and $R_H(\vec{r})$ are the spatial resolution for the case of compensated field and in the presence of the magnetic field H , respectively. $\mu(Shield)$ is the mean number of the p.e. registered in the case when the PMT is placed inside the μ - metal shielding. $I(Shield)$ is the PMT relative sensitivity in the case when the PMT is placed inside the μ - metal shielding in comparison to the case of completely compensated field.

The expected degradation of the spatial resolution is 3% in the case of a zero Y-axis component.

5 Tolerance on the PMT orientation

In the previous Sections we have understood that the \mathbf{Y} component is the most sensitive to the magnetic field. So, in an effort to minimize the effects of the EMF we have to compensate or shield the field along the \mathbf{Y} axis as much as we can. However, to study

Figure 4: PMT charge distribution against a magnetic field applied along its Y-axis. The field is measured in units of $40 \mu T$.



properly the way we get rid of this component we need to quantify how the accuracy of the alignment could affect the PMT performances.

With this in mind in this Section we investigate how the energy degradation depends upon the accuracy of the PMT orientation with respect to the EMF. In order to do that we studied the degradation of the PMT performances against a magnetic field along the **Y**- axis. The results are presented in table 3 and table 4.

The dependence of the PMT charge distribution on the field applied along its Y axis can be seen also in Figure 4.

The data reported in this Section were acquired with a different PMT, so the absolute values of the parameters are different with respect to the corresponding ones in the previous Sections.

One can see that with an accuracy in the PMT orientation of ~ 12 degrees ($H_Y \leq 0.2EMF$), both the energy resolution and the space resolution will be only 5% worse . With an accuracy of ~ 18 degrees ($H_Y \leq 0.3EMF$) the degradation will be 10%.

6 Practical issues

For the sake of completeness in this Section briefly we underline few practical issues to take into account in the case it is decided to compensate the EMF effects by the technique described above. The solution of PMTs orientation will definitely complicate the procedure of PMTs mounting in the detector. Moreover, the necessary additional steps on the pre-mounting stage are the following:

1. Marking of the PMT Y-axis during manufacturing of PMTs
2. A technical solution should be provided in order to have the possibility to rotate each PMT around its symmetry axis (Z-axis) .

The additional procedures during the PMTs assembling are:

1. Measurements of the EMF should be performed at each mounting point and corresponding field direction should be marked.
2. PMTs should be assembled keeping the marks overlapping within an angle of 10 degrees.

7 Conclusions

In this paper we have studied the possibility to align a PMT in the EMF in such a way that the degradation in the measurements of the energy and spatial resolution in a liquid scintillator detector is minimized. We have shown that for a PMT such as the 8" ETL9351 the component of the field along the \mathbf{Y} axis is the most important to compensate or shield in order to not change the PMT performances. We have also shown that with an accuracy of about 12 degrees in the alignment of the PMTs with respect to the field the energy resolution degradation could be kept within a 5%.

This is an alternative solution to the standard use of a μ -metal shielding or a coil-system. The procedure to align a huge number of PMTs could be difficult and time consuming (measurements of the EMF should be performed at each point, field direction should be labeled etc). However, we believe that depending on the detector and PMTs mounting procedure it could be worthing taking into account the quantitative results reported in this paper to install, as an example, a small fraction of PMTs which could be not mounted with μ -metals as mentioned in Section 1. Furthermore, even in the case it is decided to build a coil-system some PMTs could be located by supporting structures which makes the EMF not homogeneous enough to be properly compensated. Again in this scenario the possibility to align the PMT it could be very helpful.

References

- [1] Arpesella C. et al, Borexino at Gran Sasso - Proposal for a real time detector for low energy solar neutrino.. Volume 1.
Edited by G.Bellini, M.Campanella, D.Guigni, Dept. of Physics of the University of Milano. August 1991.
- [2] BOREXINO collaboration, G.“ Alimonti, proposal to the National Science Foundation, edited by F. P. Calaprice et al., Princeton 1996
- [3] BOREXINO collaboration, **NIM A 406 (1998)** p.411-426.
- [4] Alimonti G. et al. **Astropart. Phys. 8 (1998)** 141.
- [5] G. Bacchiocchi et al, The Earth's magnetic field compensation in the borexino phototubes facility . **INFN/TC-97/35, Nov. 7 1997**, (available at www.lngs.infn.it).
- [6] see in particular Super-Kamiokande Official Home Page at <http://www-sk.icrr.u-tokyo.ac.jp/doc/sk/index.html>.
- [7] R. Dossi, A. Ianni, R.Scardaoni, A circular coil system to compenstae magnetic field in the Borexino experiment. BOREXINO official home page at <http://almime.mi.infn.it/>.
- [8] R. Dossi, A. Ianni, G. Ranucci, O. Ju. Smirnov, Methods for precise photoelectron counting with photomultipliers, **INFN/TC-98/18, July 17 1998**, Accepted for publication on NIM A.
- [9] 97-07-02 Status Report of the PMT Working Group, G. Bachiocchi, A. Brigatti, R. Dossi, C. Galbiati, S. Grabar, A. Ianni, P. Inzani, G. Korga, P. Lombardi, G. Ranucci, E. Resconi, F. Sacchetti, R. Scardaoni, O. Smirnov, A. Sotnikov, July 1997. BOREXINO official home page at <http://almime.mi.infn.it/>.
- [10] A. Ianni and O. Smirnov, Theoretical estimation of the CTF line width using the PMT charge spectra, BOREXINO Internal note, Jan. 1998. BOREXINO official home page at <http://almime.mi.infn.it/>.
- [11] O.Smirnov, PhD thesis. Dubna, 2000. To appear as INFN preprint.